

NATURAL CONVECTION NUMERIC SIMULATION ON METAL FREEZING USING DIFFERENTIAL METHOD

Heri Suprianto¹, Eko Prasetyo B.², Purwadi Joko Widodo²

¹Student, ²Lecturer– Mechanical Engineering Department–Universitas Sebelas Maret

Keywords :

natural convection
metal solidification
finite different method
rayleigh number

Abstract :

The research of modeling of natural convection in metal solidification process with finite different method was conducted to determine temperature distribution and fluid flow profil with variations value Rayleigh number. The research conducted by solving governing equation of natural convection with finite difference approximation. Governing equation of natural convection consist of continuity equation, momentum equations, and energy equation. The ADI (Alternating Directional Implicit) method was used to discrteze for governing equation of natural convection. Finite difference method was written in Fortran language whereas the temperature distribution and fluid flow profile were visualized with Matlab software. The results of this research was validated by comparing the results obtained with Rajiv Sampath research. Comparison of the results of research showed good agreement. The result showed that solidification process occurs faster at $Ra\ 10^4$ compared with 10^5 and 10^6

1. INTRODUCTION

Numerous things related to the heat transfer are found in everyday life, especially in the field of industry. Heat transfer can occur in three ways, namely conduction, convection, and radiation.

Convection is a heat transfer that occurs between solid surface to the moved fluid which caused by the temperature difference within. Convection which is based on the fluid flow origins are categorized into two categories, namely the forced convection and natural convection.

Forced Convection is heat transfer fluid flow convection which happened influenced by external tools, such as fans, pumps, and others. While natural convection is heat transfer fluid flow convection which is caused by the differences in fluid density caused by heating and cooling.

Natural convection plays an important role in the engineering industry, one of them in the metal solidification process. Research which concerned on natural convection freezing problem is extremely crucial, because the fluid flow which caused by natural convection in liquid state, it changing the shape of the liquid/ solid interface and temperature distribution during freezing (Yinheng, 1994).

Physical phenomena that control the solid/ liquid interface shape during freezing are becoming necessary in numerous industrial processes. Its main characteristic is that the interface moves to separate the two phases with different physical properties. Differences in temperature cause the buoyancy liquid produces significant convection currents. Natural convection has a major influence on the morphology of its interface, freezing rate, and temperature distribution (Mohammad 2009).

Research about the natural convection issue of metals freezing has been carried out both experimental and numerically. Experimental laboratory research requires a significant financial cost and the process is quite complicated. Therefore, numerically study was developed which much cheaper. Various methods of numerical approach to determine the natural convection phenomenon has been done, using a mathematical model of the continuity equation, momentum equation, and energy equation.

Numerical study on natural convection issue of metal freezing was growing rapidly from year to year. McDaniel and Zabaras (1994) made a 2D numerical modeling on the basis of natural convection phase transformation on the issues of freezing and thawing of pure metals using the finite element method. Chen and Yoo (1995) analyzed the natural convection of aluminum freezing process by applying finite element method. Sampath and Zabaras (1999) created 2D and 3D numerical modeling on it utilizing the finite element method. Sampath and Zabaras research studied it on pure metals and alloys. Mohammad (2010) examined the numerical simulations in freezing water in a square mold in natural convection by employing finite volume method. Balhamadia, Kane, and Fortin (2012) made a phase transition modeling by natural convection in the water freezing and thawing gallium.

2. SCOPE

This study is aimed to make a natural convection modeling in the metal solidification process with finite difference methods. The velocity vector and temperature distribution were included.

3. LITERATURE REVIEW

McDaniel and Zabaras (1994) made a 2D numerical modeling on the basis of natural convection phase transformation on the freezing and thawing issues of pure metal using the finite element method. There were two cases analyzed. It was 105 and 106 of Rayleigh numbers. The boundary conditions that used were top, bottom, and right side insulation while the left side was the convection.

Chen and Yoo (1995) analyzed the freezing process aluminum in natural convection with the finite element method.

Sampath and Zabaras (1999) created 2D and 3D numerical modeling on the basis of natural convection phase transformation using the finite element method. Sampath and Zabaras Research investigated the freezing and thawing problem of pure metals and alloys. Basically, this study was continued by Zabaras research (1994).

Mohammad (2010) studied the numerical simulations in freezing water in a square mold in natural convection by using finite volume method. Balhamadia, Kane, and Fortin (2012) fabricated the phase transition modeling by natural convection in the water freezing and thawing gallium.

4. RESEARCH METHODOLOGY

4.1 Research Procedure

Research was done by making the program implementation to resolve the momentum equation, energy equation, and the continuity equation with the ADI method.

An outline of the research can be made following flow chart:

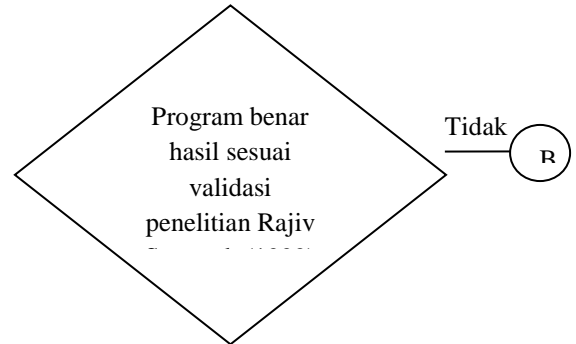
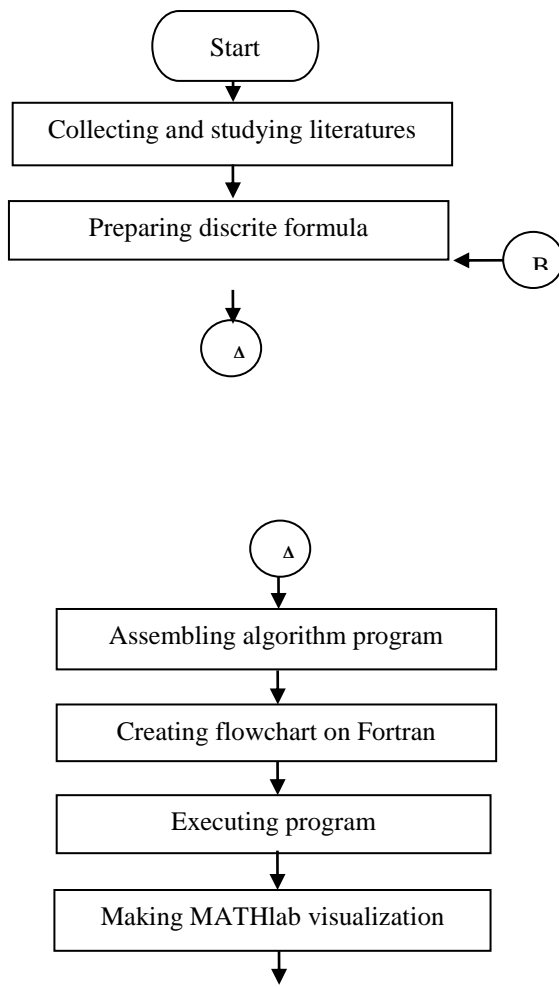


Figure 4.1. Research flowchart

4.2 Diskritisasi Persamaan Atur

Natural convection equation set consists of the continuity equation, momentum equation, and energy equation. In order to set the natural convection equations can be applied in the programming language. Firstly, discretization equation set was set up.

This study implementation, the discretization equation solved by the method set ADI. By defining $\frac{1}{2}(x_{i,j}^n + x_{i+1,j}^n) = XR$, $\frac{1}{2}(x_{i,j}^n + x_{i-1,j}^n) = XL$, $\frac{1}{2}(x_{i,j}^n + x_{i,j+1}^n) = XT$, $\frac{1}{2}(x_{i,j}^n + x_{i,j-1}^n) = XB$ where x is unknown variable (such as, u , v , and θ).

4.2.1 Momentum Equation Discrete

4.2.1.1 X-axis Momentum Equation

Discretization of momentum equation used x-axis momentum equation x direction without including the pressure element. Therefore, the equation becomes:

$$\frac{\partial u}{\partial t} + u \frac{\partial u}{\partial x} + v \frac{\partial u}{\partial y} = \frac{Pr}{Ra^{0.5}} \left(\frac{\partial^2 u}{\partial x^2} + \frac{\partial^2 u}{\partial y^2} \right) + Pr \theta \cos \theta$$

For example $= \frac{Pr}{Ra^{0.5}}$, so, the equation above become,

$$\frac{\partial u}{\partial t} + u \frac{\partial u}{\partial x} + v \frac{\partial u}{\partial y} = A \left(\frac{\partial^2 u}{\partial x^2} + \frac{\partial^2 u}{\partial y^2} \right) + \text{Pr} \theta \cos \phi$$

a. X-Sweep

X-sweep equation for momentum equation x-axis is

$$\frac{\partial u}{\partial t} + u \frac{\partial u}{\partial x} + A \frac{\partial^2 u}{\partial x^2} = -v \frac{\partial u}{\partial y} + A \frac{\partial^2 u}{\partial y^2} + \text{Pr} \theta \cos \phi$$

Discretization for each equation above can be explained:

$$\begin{aligned} \diamond \frac{\partial u}{\partial t} &= \frac{u_{i,j}^{n+1/2} - u_{i,j}^n}{\frac{\Delta t}{2}} \\ \diamond u \frac{\partial u}{\partial x} &= \frac{1}{2\Delta x} \left[\text{UR} \cdot u_{i+1,j}^{n+1/2} + (\text{UR} - \text{UL}) u_{i,j}^{n+1/2} + \text{UL} \cdot u_{i-1,j}^{n+1/2} \right] \\ \diamond \frac{\partial^2 u}{\partial x^2} &= \frac{u_{i+1,j}^{n+1/2} - 2u_{i,j}^{n+1/2} + u_{i-1,j}^{n+1/2}}{\Delta x^2} \\ \diamond v \frac{\partial u}{\partial y} &= \frac{1}{\Delta y} [\text{VT} \cdot \text{UT} - \text{VB} \cdot \text{UB}] \\ \diamond \frac{\partial^2 u}{\partial y^2} &= \frac{u_{i,j+1}^n - 2u_{i,j}^n + u_{i,j-1}^n}{\Delta y^2} \end{aligned}$$

By substituting equations above and multiplying with $\frac{\Delta t}{2}$, can be obtained:

$$\begin{aligned} u_{i,j}^{n+1/2} - u_{i,j}^n + \frac{\Delta t}{4\Delta x} \left[\text{UR} \cdot u_{i+1,j}^{n+1/2} + (\text{UR} - \text{UL}) u_{i,j}^{n+1/2} + \text{UL} \cdot u_{i-1,j}^{n+1/2} \right] \\ - \frac{A\Delta t}{2\Delta x^2} \left[u_{i+1,j}^{n+1/2} - 2u_{i,j}^{n+1/2} + u_{i-1,j}^{n+1/2} \right] = - \frac{\Delta t}{2\Delta y} [\text{VT} \cdot \text{UT} - \text{VB} \cdot \text{UB}] \\ + \frac{A\Delta t}{2\Delta y^2} (u_{i,j+1}^n - 2u_{i,j}^n + u_{i,j-1}^n) + \frac{\Delta t}{2} \text{Pr} \cdot \theta \cdot \cos \phi \end{aligned}$$

Therefore those equations, would be collected into unknown variable on left side and known variable on right side:

$$\begin{aligned} u_{i-1,j}^{n+1/2} \left[\frac{\Delta t}{4\Delta x} \text{UL} - \frac{A\Delta t}{2\Delta x^2} \right] + u_{i,j}^{n+1/2} \left[1 + \frac{\Delta t}{4\Delta x} (\text{UR} - \text{UL}) + \frac{A\Delta t}{2\Delta x^2} \right] \\ = u_{i,j}^n - \frac{\Delta t}{2\Delta y} (\text{VT} \cdot \text{UT} - \text{VB} \cdot \text{UB}) + \frac{A\Delta t}{2\Delta y^2} (u_{i,j+1}^n - 2u_{i,j}^n + u_{i,j-1}^n) \\ + \frac{\Delta t}{2} \text{Pr} \cdot \theta \cdot \cos \phi \end{aligned}$$

Arrangement above idencally with equation $a_i u_{i-1,j}^{n+1/2} + b_i u_{i,j}^{n+1/2} + c_i u_{i+1,j}^{n+1/2} = d_i$ with components a_i , b_i , c_i and d_i each is tridiagonal matrix components where:

$$\begin{aligned} a_i &= \frac{\Delta t}{2\Delta x} \left[\frac{\text{UL}}{2} + \frac{A}{\Delta x} \right] \\ b_i &= \left[1 + \frac{\Delta t}{4\Delta x} (\text{UR} - \text{UL}) + \frac{A\Delta t}{2\Delta x^2} \right] \\ c_i &= \frac{\Delta t}{2\Delta x} \left[\frac{\text{UR}}{2} - \frac{A}{\Delta x} \right] \\ d_i &= u_{i,j}^n - \frac{\Delta t}{2\Delta y} (\text{VT} \cdot \text{UT} - \text{VB} \cdot \text{UB}) \\ &+ \frac{A\Delta t}{2\Delta y^2} (u_{i,j+1}^n - 2u_{i,j}^n + u_{i,j-1}^n) + \frac{\Delta t}{2} \text{Pr} \cdot \theta \cdot \cos \phi \end{aligned}$$

b. Y-Sweep

Y-sweep equation for momentum equation y-axis is:

$$\frac{\partial u}{\partial t} + v \frac{\partial u}{\partial x} + A \frac{\partial^2 u}{\partial y^2} = -u \frac{\partial u}{\partial x} + A \frac{\partial^2 u}{\partial x^2} + \text{Pr} \theta \cos \phi$$

Discretization for each equation above can be explained:

$$\begin{aligned} \diamond \frac{\partial u}{\partial t} &= \frac{u_{i,j}^{n+1} - u_{i,j}^{n+1/2}}{\frac{\Delta t}{2}} \\ \diamond v \frac{\partial u}{\partial x} &= \frac{1}{2\Delta y} \left[\text{VT} \cdot u_{i+1,j}^{n+1} + (\text{VT} - \text{VB}) u_{i,j}^{n+1} + \text{VB} \cdot u_{i-1,j}^{n+1} \right] \\ \diamond \frac{\partial^2 u}{\partial y^2} &= \frac{u_{i,j+1}^{n+1} - 2u_{i,j}^{n+1} + u_{i,j-1}^{n+1}}{\Delta y^2} \\ \diamond u \frac{\partial u}{\partial y} &= \frac{1}{\Delta x} [\text{UR}^2 - \text{UL}^2] \\ \diamond \frac{\partial^2 u}{\partial x^2} &= \frac{u_{i,j+1}^{n+1/2} - 2u_{i,j}^{n+1/2} + u_{i,j-1}^{n+1/2}}{\Delta x^2} \end{aligned}$$

By substituting equations above and multiplying with $\frac{\Delta t}{2}$, can be obtained matrix tridiagonal coefficient:

$$\begin{aligned} a_j &= \frac{\Delta t}{2\Delta y} \left[\frac{\text{VB}}{2} + \frac{A}{\Delta x} \right] \\ b_j &= \left[1 + \frac{\Delta t}{4\Delta y} (\text{VT} - \text{VB}) + \frac{A\Delta t}{2\Delta y^2} \right] \\ c_j &= \frac{\Delta t}{2\Delta y} \left[\frac{\text{VB}}{2} - \frac{A}{\Delta y} \right] \\ d_i &= u_{i,j}^{n+1/2} - \frac{\Delta t}{2\Delta x} (\text{UR}^2 - \text{UL}^2) \\ &+ \frac{A\Delta t}{2\Delta x^2} (u_{i,j+1}^{n+1/2} - 2u_{i,j}^{n+1/2} + u_{i,j-1}^{n+1/2}) + \frac{\Delta t}{2} \text{Pr} \cdot \theta \cdot \cos \phi \end{aligned}$$

4.2.1.2 Y-axis Momentum Equation

Discretization of momentum equation used y-axis momentum equation y direction without including the pressure element. Therefore, the equation becomes:

$$\frac{\partial v}{\partial t} + u \frac{\partial v}{\partial x} + v \frac{\partial v}{\partial y} = \frac{\text{Pr}}{\text{Ra}^{0.5}} \left(\frac{\partial^2 v}{\partial x^2} + \frac{\partial^2 v}{\partial y^2} \right) + \text{Pr} \theta \cos \phi$$

For example $A = \frac{\text{Pr}}{\text{Ra}^{0.5}}$, so, the equation above becomes:

$$\frac{\partial v}{\partial t} + u \frac{\partial v}{\partial x} + v \frac{\partial v}{\partial y} = A \left(\frac{\partial^2 v}{\partial x^2} + \frac{\partial^2 v}{\partial y^2} \right) + \text{Pr} \theta \cos \phi$$

a. X-Sweep

X-sweep equation for momentum equation x-axis is:

$$\frac{\partial v}{\partial t} + u \frac{\partial v}{\partial x} + A \frac{\partial^2 v}{\partial x^2} = -v \frac{\partial v}{\partial y} + A \frac{\partial^2 v}{\partial y^2} + \text{Pr} \theta \cos \phi$$

Discretization for each equation above can be explained:

$$\begin{aligned} \diamond \frac{\partial v}{\partial t} &= \frac{v_{i,j}^{n+1/2} - v_{i,j}^n}{\frac{\Delta t}{2}} \\ \diamond u \frac{\partial v}{\partial x} &= \frac{1}{2\Delta x} \left[\text{UR} \cdot v_{i+1,j}^{n+1/2} + (\text{UR} - \text{UL}) v_{i,j}^{n+1/2} + \text{UL} \cdot v_{i-1,j}^{n+1/2} \right] \\ \diamond \frac{\partial^2 v}{\partial x^2} &= \frac{v_{i+1,j}^{n+1/2} - 2v_{i,j}^{n+1/2} + v_{i-1,j}^{n+1/2}}{\Delta x^2} \\ \diamond v \frac{\partial v}{\partial y} &= \frac{1}{\Delta y} [\text{VT}^2 - \text{VB}^2] \\ \diamond \frac{\partial^2 v}{\partial y^2} &= \frac{v_{i,j+1}^n - 2v_{i,j}^n + v_{i,j-1}^n}{\Delta y^2} \end{aligned}$$

By substituting equations above and multiplying with $\frac{\Delta t}{2}$, can be obtained: tridiagonal matrix coefficient:

$$\begin{aligned} a_i &= \frac{\Delta t}{2\Delta x} \left[\frac{UL}{2} + \frac{A}{\Delta x} \right] \\ b_i &= \left[1 + \frac{\Delta t}{4\Delta x} (UR-UL) + \frac{A\Delta t}{2\Delta x^2} \right] \\ c_i &= \frac{\Delta t}{2\Delta x} \left[\frac{UR}{2} - \frac{A}{\Delta x} \right] \\ d_i &= v_{ij}^n - \frac{\Delta t}{2\Delta y} (VT^2 - VB^2) \\ &\quad + \frac{A\Delta t}{2\Delta y^2} (v_{ij+1}^n - 2v_{ij}^n + v_{ij-1}^n) + \frac{\Delta t}{2} Pr \cdot \theta \cdot \cos\phi \end{aligned}$$

b. Y-Sweep

Y-sweep equation for momentum equation y-axis is:

$$\frac{\partial v}{\partial t} + v \frac{\partial v}{\partial x} + A \frac{\partial^2 v}{\partial y^2} = -u \frac{\partial v}{\partial y} + A \frac{\partial^2 v}{\partial x^2} + Pr\theta \cos\phi$$

Discretization for each equation above can be explained:

$$\begin{aligned} \diamond \frac{\partial v}{\partial t} &= \frac{v_{ij}^{n+1} - v_{ij}^{n+1/2}}{\frac{\Delta t}{2}} \\ \diamond v \frac{\partial v}{\partial x} &= \frac{1}{2\Delta y} \left[VT \cdot v_{i+1,j}^{n+1} + (VT-VB)v_{ij}^{n+1} + VB \cdot v_{i-1,j}^{n+1} \right] \\ \diamond \frac{\partial^2 v}{\partial y^2} &= \frac{v_{i+1,j}^{n+1} - 2v_{ij}^{n+1} + v_{i-1,j}^{n+1}}{\Delta y^2} \\ \diamond u \frac{\partial v}{\partial y} &= \frac{1}{\Delta x} [UR \cdot VR - UL \cdot VL] \\ \diamond \frac{\partial^2 v}{\partial x^2} &= \frac{v_{ij+1}^{n+1/2} - 2v_{ij}^{n+1/2} + v_{ij-1}^{n+1/2}}{\Delta x^2} \end{aligned}$$

By substituting equations above and multiplying with $\frac{\Delta t}{2}$, can be obtained matrix tridiagonal coefficient:

$$\begin{aligned} a_j &= \frac{\Delta t}{2\Delta y} \left[\frac{VB}{2} + \frac{A}{\Delta x} \right] \\ b_j &= \left[1 + \frac{\Delta t}{4\Delta y} (VT-VB) + \frac{A\Delta t}{2\Delta y^2} \right] \\ c_j &= \frac{\Delta t}{2\Delta y} \left[\frac{VB}{2} - \frac{A}{\Delta x} \right] \\ d_i &= u_{i,j}^{n+1/2} - \frac{\Delta t}{2\Delta x} (UR \cdot VR - UL \cdot VL) \\ &\quad + \frac{A\Delta t}{2\Delta x^2} (v_{ij+1}^{n+1/2} - 2v_{ij}^{n+1/2} + v_{ij-1}^{n+1/2}) + \frac{\Delta t}{2} Pr \cdot \theta \cdot \cos\phi \end{aligned}$$

4.2.2 Pressure Iteration Using Line Gauss Seidel

Formula was used to calculate pressure is:

$$\frac{\partial^2 p}{\partial x^2} + \frac{\partial^2 p}{\partial y^2} = \frac{1}{\Delta t} \left(\frac{\partial u}{\partial x} + \frac{\partial v}{\partial y} \right)$$

Discretization for each equations above:

$$\begin{aligned} \diamond \frac{\partial^2 p}{\partial x^2} &= \frac{p_{i+1,j} - 2p_{ij} + p_{i-1,j}}{\Delta x^2} \\ \diamond \frac{\partial^2 p}{\partial y^2} &= \frac{p_{i,j+1} - 2p_{ij} + p_{i,j-1}}{\Delta y^2} \end{aligned}$$

$$\diamond \frac{\partial u}{\partial x} = \frac{u_{i+1,j} - u_{i-1,j}}{2\Delta x}$$

$$\diamond \frac{\partial v}{\partial y} = \frac{v_{i+1,j} - v_{i-1,j}}{2\Delta y}$$

By substituting equations above, so tridiagonal matrix coefficient can be obtained:

$$a_i = 1$$

$$b_i = -4$$

$$c_i = 1$$

$$d_i = -p_{i,j+1} - p_{i,j-1} + \frac{\Delta x^2}{\Delta t} \left[\frac{u_{i+1,j} - u_{i-1,j}}{2\Delta x} + \frac{v_{i+1,j} - v_{i-1,j}}{2\Delta y} \right]$$

4.2.3 Energy Discretization Equation

Energy discretization equation was used:

$$\frac{\partial \theta}{\partial t} + u \frac{\partial \theta}{\partial x} + v \frac{\partial \theta}{\partial y} = \frac{1}{Ra^{0.5}} \left(\frac{\partial^2 \theta}{\partial x^2} + \frac{\partial^2 \theta}{\partial y^2} \right)$$

For example $= \frac{1}{Ra^{0.5}}$, so, the equation above becomes:

$$\frac{\partial \theta}{\partial t} + u \frac{\partial \theta}{\partial x} + v \frac{\partial \theta}{\partial y} = B \left(\frac{\partial^2 \theta}{\partial x^2} + \frac{\partial^2 \theta}{\partial y^2} \right)$$

From those equations above, could produce discretization:

a. X-Sweep

X-sweep equation for momentum equation x-axis is

$$\frac{\partial \theta}{\partial t} + u \frac{\partial \theta}{\partial x} + B \frac{\partial^2 \theta}{\partial x^2} = -v \frac{\partial \theta}{\partial y} + B \frac{\partial^2 \theta}{\partial y^2}$$

Discretization for each equation above can be explained:

$$\begin{aligned} \diamond \frac{\partial \theta}{\partial t} &= \frac{\theta_{ij}^{n+1/2} - \theta_{ij}^n}{\frac{\Delta t}{2}} \\ \diamond u \frac{\partial \theta}{\partial x} &= \frac{1}{2\Delta x} \left[UR \cdot \theta_{i+1,j}^{n+1/2} + (UR-UL)\theta_{ij}^{n+1/2} + UL \cdot \theta_{i-1,j}^{n+1/2} \right] \\ \diamond \frac{\partial^2 \theta}{\partial x^2} &= \frac{\theta_{i+1,j}^{n+1/2} - 2\theta_{ij}^{n+1/2} + \theta_{i-1,j}^{n+1/2}}{\Delta x^2} \\ \diamond v \frac{\partial \theta}{\partial y} &= \frac{1}{\Delta y} [VT \cdot \theta_{i,j} - VB \cdot \theta_{i,j}] \\ \diamond \frac{\partial^2 \theta}{\partial y^2} &= \frac{\theta_{i,j+1}^n - 2\theta_{ij}^n + \theta_{i,j-1}^n}{\Delta y^2} \end{aligned}$$

By substituting equations above and multiplying with $\frac{\Delta t}{2}$, can be obtained: tridiagonal matrix coefficient:

$$\begin{aligned} a_i &= \frac{\Delta t}{2\Delta x} \left[\frac{UL}{2} + \frac{B}{\Delta x} \right] \\ b_i &= \left[1 + \frac{\Delta t}{4\Delta x} (UR-UL) + \frac{B\Delta t}{2\Delta x^2} \right] \\ c_i &= \frac{\Delta t}{2\Delta x} \left[\frac{UR}{2} - \frac{B}{\Delta x} \right] \\ d_i &= \theta_{ij}^n - \frac{\Delta t}{2\Delta y} (VT \cdot \theta_{i,j} - VB \cdot \theta_{i,j}) + \frac{B\Delta t}{2\Delta y^2} (\theta_{i,j+1}^n - 2\theta_{ij}^n + \theta_{i,j-1}^n) \end{aligned}$$

b. Y-Sweep

Y-sweep equation for momentum equation y-axis is

$$\frac{\partial \theta}{\partial t} + v \frac{\partial \theta}{\partial x} + B \frac{\partial^2 \theta}{\partial x^2} = -u \frac{\partial \theta}{\partial y} + B \frac{\partial^2 \theta}{\partial y^2}$$

Y-sweep equation for momentum equation y-axis is:

$$\diamond \frac{\partial \theta}{\partial t} = \frac{\theta_{ij}^{n+1} - \theta_{ij}^{n+1/2}}{\frac{\Delta t}{2}}$$

$$\begin{aligned} \diamond v \frac{\partial \theta}{\partial y} &= \frac{1}{2\Delta y} [VT.\theta_{i+1,j}^{n+1} + (VT-VB)\theta_{i,j}^{n+1} + VB.\theta_{i-1,j}^{n+1}] \\ \diamond \frac{\partial^2 \theta}{\partial y^2} &= \frac{\theta_{i,j+1}^{n+1} - 2\theta_{i,j}^{n+1} + \theta_{i,j-1}^{n+1}}{\Delta y^2} \\ \diamond u \frac{\partial \theta}{\partial x} &= \frac{1}{\Delta x} [UR.\theta R - UL.\theta L] \\ \diamond \frac{\partial^2 \theta}{\partial x^2} &= \frac{\theta_{i+1,j}^{n+1/2} - 2\theta_{i,j}^{n+1/2} + \theta_{i-1,j}^{n+1/2}}{\Delta x^2} \end{aligned}$$

By substituting equations above and multiplying with $\frac{\Delta t}{2}$, can be obtained matrix tridiagonal coefficient::

$$\begin{aligned} a_i &= \frac{\Delta t}{2\Delta y} \left[\frac{UL}{2} + \frac{B}{\Delta y} \right] \\ b_i &= \left[1 + \frac{\Delta t}{4\Delta y} (VT-VB) + \frac{B\Delta t}{2\Delta y^2} \right] \\ c_i &= \frac{\Delta t}{2\Delta y} \left[\frac{VB}{2} - \frac{B}{\Delta y} \right] \\ d_i &= \theta_{i,j}^{n+1/2} - \frac{\Delta t}{2\Delta x} (UR.\theta R - UL.\theta L) \\ &\quad + \frac{B\Delta t}{2\Delta x^2} (\theta_{i,j+1}^{n+1/2} - 2\theta_{i,j}^{n+1/2} + \theta_{i,j-1}^{n+1/2}) \end{aligned}$$

5. RESULT AND DISCUSSION

5.1 Program Validation

Validation program was done by comparing the current research to the Rajiv Sampath research (1999). Rajiv Sampath research domain (1999) was the resolution of natural convection case in metal solidification process on a square mold with 1: 1 of aspect ratio, with the walls below, above, and right side condition were insulating, while the left Wall was convection.

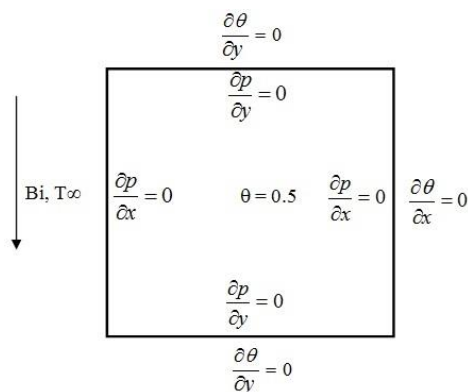


Figure 5.1 Boundary and required research condition

Rajiv Sampath research (1999) was using finite element method with the same boundary conditions to the present study boundary conditions. Isothermal visualization and velocity vector results will be compared with Rajiv Sampath research (1999) at $Ra = 105$. Isothermal comparison results is shown in following Table 4.1. and Table 4.2:

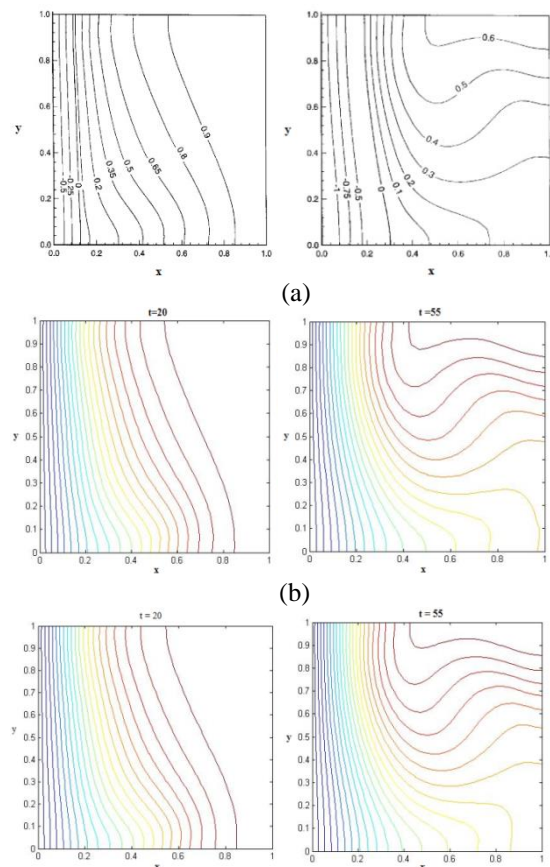
Table 4. 1. Isothermal comparison result at $t=20$

Titik		Sekarang		Beda (%)	Sampath	Beda (%)	
x	Y	Grid 61x61	Grid 81x81			61x61	81x81
0.53	0.1	0.52931	0.50247	5.342	0.5	5.862	0.494
0.5	0.3	0.65937	0.65371	0.866	0.65	1.442	0.571
0.7	0.2	0.82506	0.81854	0.797	0.8	3.133	2.318
0.8	0.3	0.92896	0.92603	0.316	0.9	3.218	2.892

Table 4.2. Isothermal comparison result at $t=55$

Titik		Sekarang		Beda (%)	Sampath	Beda (%)	
x	Y	Grid 61x61	Grid 81x81			61x61	81x81
0.6	0.3	0.30965	0.30485	1.575	0.3	3.217	1.617
1.0	0.63	0.41458	0.39613	4.658	0.4	3.645	0.968
0.4	0.68	0.5161	0.50969	1.258	0.5	3.22	1.938
1.0	0.87	0.61367	0.60215	1.913	0.6	2.278	0.358

Isothermal comparison results between the current study to Sampath research above shows good accuracy with 5862 for the 61x61 grid and 2892 for 81x81 of a maximum error. It shows for the 81x81 grid has a maximum error value is smaller than the 61x61 grid, so that in this study we used the 81x81 grid. Visualization comparison of nowadays research with Sampath research above can be shown in the following figure:



(c)
Figure 5.2 Isothermal visualization comparison at $Ra=10^5$ (a) Rajiv Sampath research (1999) (b) Nowadays research with 61x61 grid (c) with 81x81 grid

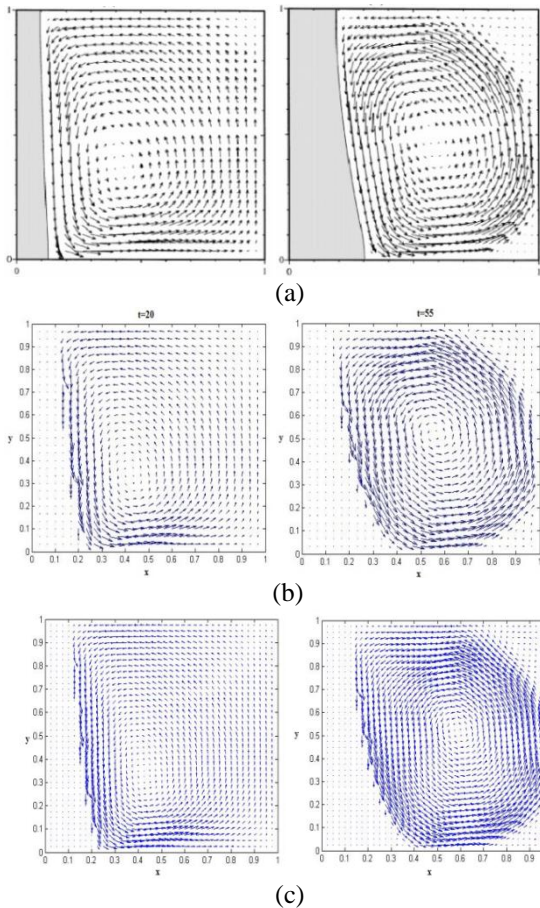


Figure 5.3. Visualization comparison velocity vector at $Ra=10^5$ (a) Rajiv Sampath research (1999) (b) Nowadays research with 61x61 grid (c) with 81x81 grid

Visually, nowadays research shows similarities of flow temperature distribution and velocity with Rajiv Sampath study (1999). Therefore, it can be said using the finite difference method has a good fit.

5.2 Natural Convection Simulation on Metal Solidification Process

Natural convection simulation cases on metal solidification process on a square mold is shown with the 81x81 grid, 0.0149 of Prandtl number (Pr), and $dt=0.001$ of time step, and Rayleigh number (Ra) variations were 104.105 and 106. The simulation results can be seen in the following image:

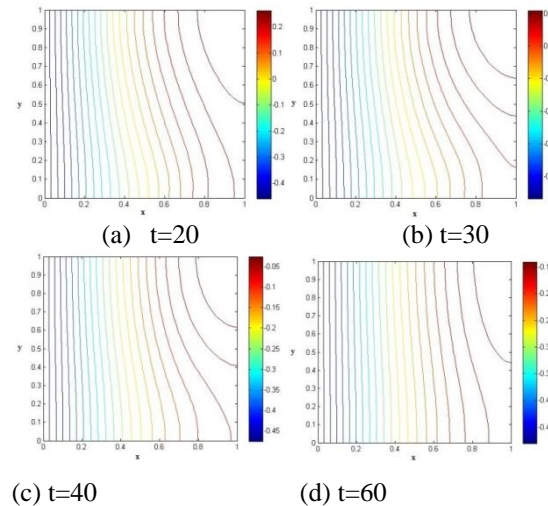


Figure 5.4. Isothermal on $Ra=10^4$

Temperature tranformation can be seen in the temperature distribution graph which represented by a point $(x, 0.1)$, wherein x were 0.1, 0.2, 0.3, 0.4, 0.5, 0.6, 0.7, 0.8, 0.9, and 1. A temperature distribution graph is as follows:

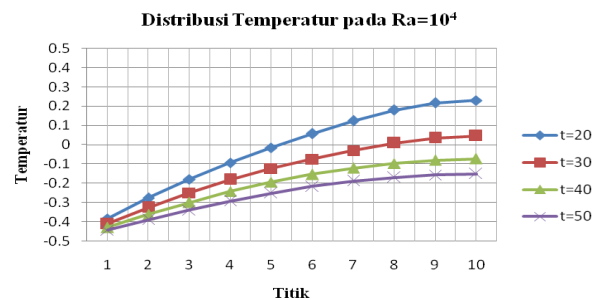


Figure 5.5. Temperature distribution at $Ra=10^4$

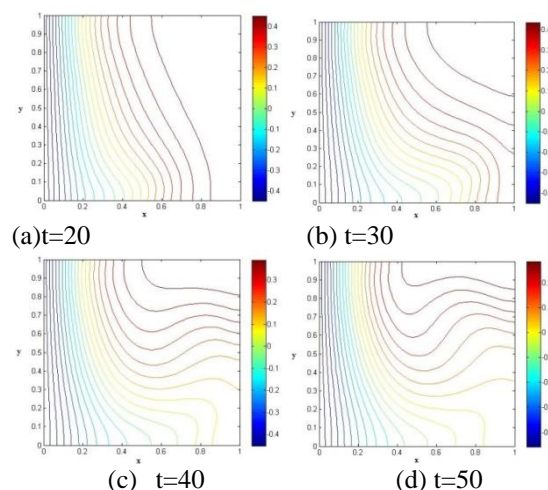
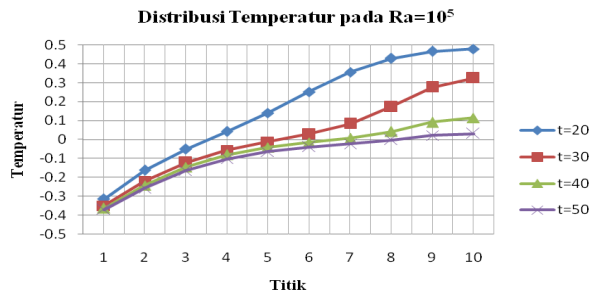
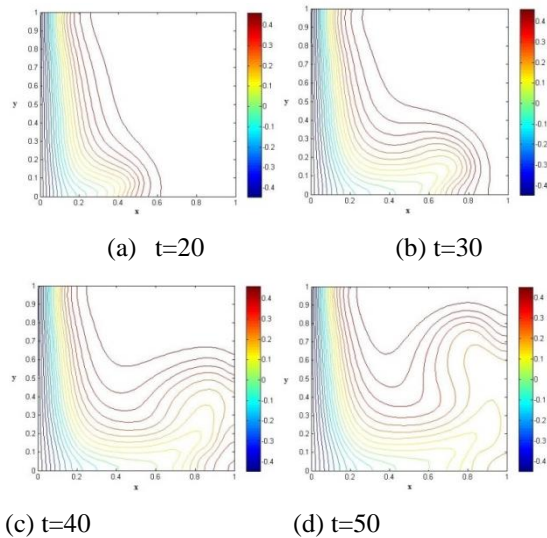
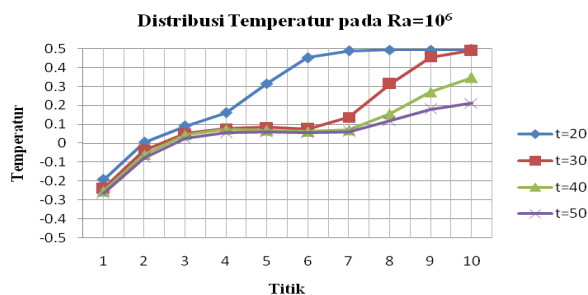


Figure 5.6. Isothermal at $Ra=10^5$

Temperature distribution can be seen in the temperature distribution graph which performed by a point $(x, 0.1)$, wherein x is 0.1, 0.2, 0.3, 0.4, 0.5, 0.6, 0.7, 0.8, 0.9, and 1. Temperature distribution graph is as follows:

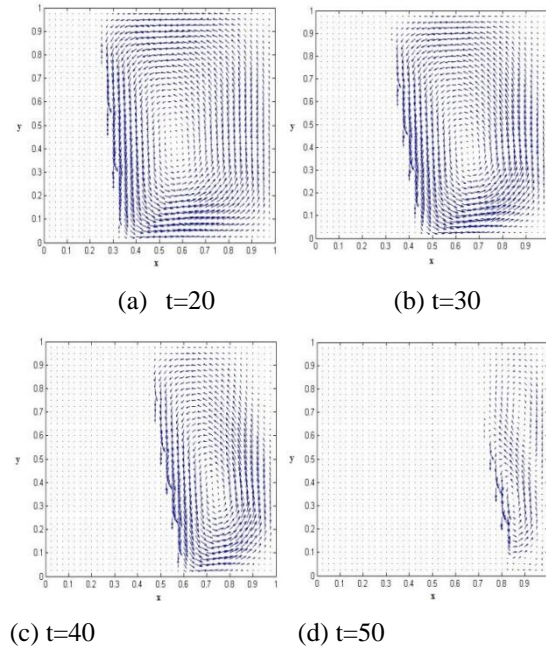
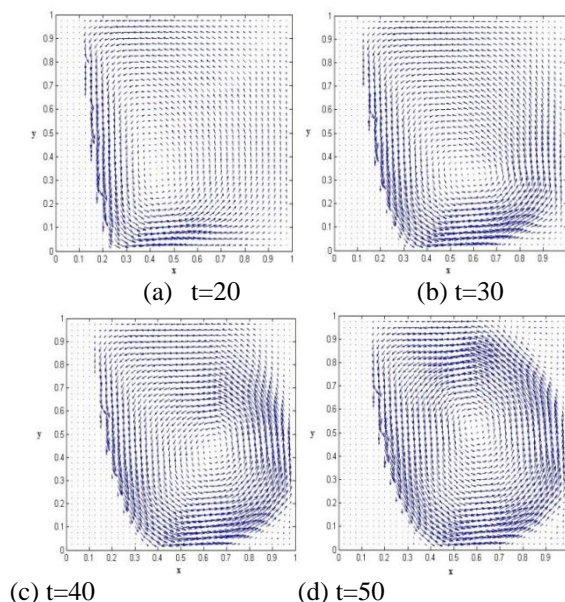
Figure 5.7. Temperature distribution at $Ra = 10^5$ Figure 5.8. Isothermal at $Ra = 10^6$

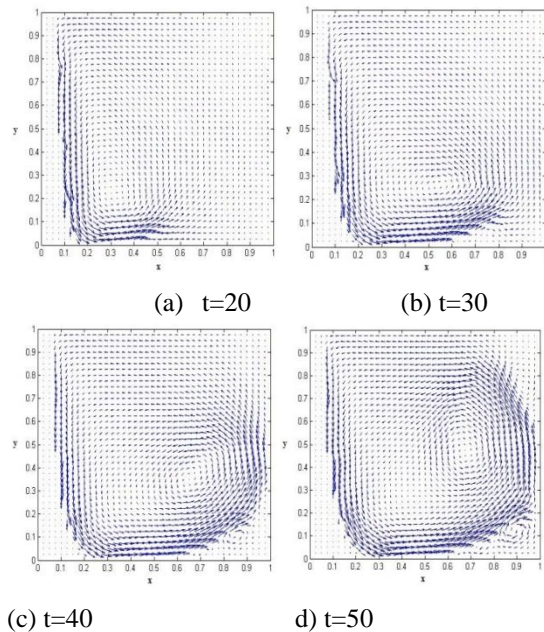
Temperature transformation can be seen in the temperature distribution graph which served by a point $(x, 0.1)$, wherein x is 0.1, 0.2, 0.3, 0.4, 0.5, 0.6, 0.7, 0.8, 0.9, and 1. Temperature distribution graph is as follows:

Figure 5.9. Temperature distribution at $Ra = 10^6$

Isothermal plot results in Figure 4.4, Figure 4.6, and Figure 4.8 portrays the temperature distribution visually. Figure 4.4 at $Ra = 104$ displays that the cold fluid moves down and the hot fluid moving upwards. Cold fluid movement influenced their gravity and density changes due to its temperature changes which is producing the density increased, while the hot fluid movement was affected by buoyant force because it has a smaller density than the cold fluid. Fluid temperature near the left wall was strongly influenced by the ambient temperature.

This also occurred on $Ra = 105$ and 106 which shown in Figure 4.6 and Figure 4.8. Isothermal figure which can be seen that the fluid movement on the wall to get the cooling fluid density will be increased. The fluid density escalation caused the fluid to move downwards, while the fluid has a lower density will move upwards. Fluid movement downward was also influenced by gravity however fluid movement upward influenced by their buoyancy occurs due to it has a smaller density.

Figure 5.10. Velocity vector at $Re = 10^4$ Figure 5.11. Velocity vector at $Ra = 10^5$

Figure 5.12. Velocity vector at $Ra = 10^6$

Velocity vector visual results with the velocity vector variation can be seen in Figure Ra 4:10 to 4:12. It portrays that the fluid movement opposite to clockwise and freezing the bottom left looks faster. It also illustrates that the cold fluid moves down and the hot fluid moving upwards. Cold fluid movement was influenced by their gravity and density changes due to its temperature changes which was generated by density increased, while hot fluid movement was affected by buoyancy force.

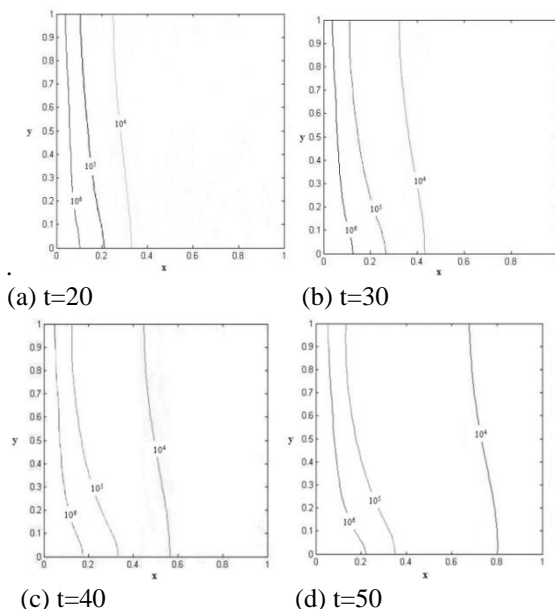


Figure 5.13. The initial solidification comparison

The initial solidification comparison which according to the Ra variations can be seen in Figure 4.13. It portrays that the initial freezing at $Ra = 104$ is faster than $Ra = 105$ and 106 . It can be concluded that

rayleigh number greatly affects the freezing process, the greater rayleigh number the longer it will reverse the freezing process so shall.

6. Conclusion

From this research and discussion that has been done. It produced a numerous conclusions:

- Research comparison of Rajiv Sampath study (1999) for natural convection problem in metal solidification process on a square mold indicates that the method which was used in this study can provide acceptable results in those cases.
- Cold fluid moved down and the hot fluid moving upwards. Cold fluid movement was influenced by their gravity and density changes due to its temperature transformation which caused the density went up, while the movement of hot fluid was affected by Buoyancy force due to it has a smaller density than the cold fluid.
- Rayleigh number greatly affects the metal solidification speed. The smaller of Rayleigh, the faster the solidification process and the greater Rayleigh number clots more slowly.

7. Reference

- Belhamadia, Y., Kane, A.S., Fortin, A., 2012, *An Enhanced Mathematical Model for Phase Change Problem With Natural Convection*, International Journal of Numerical Analysis and Modeling, Vol.3, 192-206.
- Brandes, E.A., Brook, G.B., 1992, *Smithells Metals Reference Book, 7th edition*, Butterworth-Heinemann, Oxford.
- Cengel, A.Y., 2008, *Heat Transfer A Practical Approach Second Edition*, McGraw-Hill, New York.
- Chen, Y., Im, Y.T., Yoo, J., 1995, *Finite Element Analysis of Solidification of Aluminum with Natural Convection*, Journal of Material Processing Technology, Vol.52, 592-609, Elsevier.
- Hoffman, K.A., 2000, *Computation Fluid Dynamics For Engineering Volume I*, Engineering System™, Kansas USA.
- Holman, J.P., 2010, *Heat Transfer Tenth Edition*, McGraw-Hill, New York.
- Incropera, F.M., 1996, *Introduction to Heat Transfer*, John Wiley & Sons, USA.
- McDaniel, D. J., Zabaras, N., 1994, *A least-squares front-tracking finite element method analysis of phase change with natural convection*, International Journal Numerical Method Engineering, Vol. 37, 2755-2777.